ELSEVIER

Chemical Engineering Journal 127 (2007) 47–57

Chemical Engineering Journal

www.elsevier.com/locate/cej

Experimental behaviour and design model of a fluidized bed reactor with immobilized peroxidase for phenol removal

José L. Gómez *, Antonio Bódalo, Elisa Gómez, Asunción M. Hidalgo, María Gómez, M. Dolores Murcia

Chemical Engineering Department, University of Murcia, Campus de Espinardo, 30071 Murcia, Spain

Received 6 July 2006; received in revised form 20 September 2006; accepted 23 September 2006

Abstract

In this work, immobilized derivatives of soybean peroxidase, covalently bound to glass supports with different surface areas, were used in a laboratory scale fluidized bed reactor to study their viability for use in phenol removal. The influence of the different operational variables on the process was also studied. When derivatives immobilized on supports with the highest surface area were used, 80% removal was achieved.

Since knowledge of the removal process in the fluidized bed reactor and its simulation is vital before a continuous industrial scale process can be proposed, a reactor model based on the experimental results that predicts the system's behaviour both in steady and transient state was developed. The model considers the fluidized bed reactor as a plug flow reactor in series with an ideal mixer and follows a kinetic law based on the observed external mass transfer resistances in order to work out the process rate.

The values of the model parameters were obtained by fitting phenol conversion values obtained experimentally to the model, using the CurveExpert, V 1.3, software.

The good agreement obtained between the experimental and calculated values of phenol conversion demonstrates that the model is valid as a predictive model for using this reactor configuration.

Keywords: Fluidized bed; Design model; Soybean peroxidase; Immobilized peroxidase; Phenol removal

1. Introduction

Phenolic compounds are among the most ubiquitous pollutants and they are widely known to be toxic and difficult to degrade. They are usually found in the wastewaters of numerous industries, such as the pulp and paper, wood, steel and metals, petroleum refining, resins and plastic based industries [1–4].

Biological degradation with microorganisms and adsorption and biotreatment in active carbon in different reactor configurations have been the most widely used technologies until now for the purification of industrial effluents containing phenolic products.

Several authors have described the use of fluidized bed reactors with granulated active carbon acting as both the adsorbent of phenolic products and as support for phenol-degrading microorganisms [5–8].

Fluidized beds with microorganisms immobilized on different supports have also been used for removing phenol from wastewaters. Hirata et al. [9], described the kinetics of the biological treatment of phenolic wastewaters in this type of reactor containing biofilms and suspended sludge. For highly polluted phenolic waters, Loh et al. [10], used an air lift fluidized bed reactor with *Pseudomonas putida* immobilized on pellets of expanded polyestyrene, concluding that biodegradation was limited by oxygen transfer. Working with this reactor configuration, Juárez-Ramírez et al. [11], studied the kinetics of phenol degradation with *Candida tropicalis* immobilized on agar gel, finding that the degradation rate is higher than that obtained with the free cells. A comparative study of tank and fluidized bed reactors for phenol biodegradation was made by González et al. [12], the latter enabling better control of the process and needing shorter hydraulic residence times. Furthermore, using the same type of immobilized microorganism, *Pseudomonas putida*, González

* Corresponding author. Tel.: +34 968 367351; fax: +34 968 364148.
E-mail address: carrasco@um.es (J.L. Gómez).

1385-8947/$ – see front matter © 2006 Elsevier B.V. All rights reserved.
doi:10.1016/j.cej.2006.09.021

Nomenclature

a	parameter defined in Eq. (39)
a_s	specific surface area (cm^2/g)
A	normal section of bed (cm^2)
b	parameter defined in Eq. (39)
C	bulk substrate concentration (mM)
C_L	substrate concentration at the end of fluidized zone (mM)
C_M	substrate concentration in the mixing zone (mM)
C_0	substrate concentration in the feed (mM)
C^*	substrate concentration upon particle surface (mM)
f	auxiliary function defined in Eq. (15)
F	feed flow rate (ml/min)
k	rate constant defined in Eq. (4) (min^{-1})
k_L	mass transfer coefficient (g/cm^2 min)
L	length of fluidized zone (cm)
L_f	length of initial fixed bed (cm)
p	Laplace variable
r	rate reaction (mM/min)
R	regression coefficient
s	Laplace variable
S.D.	standard deviation
t	time (min)
U	step function with a dead time
v	variable defined in Eq. (4) (cm/min)
V_M	mixing zone volume (cm^3)
x	phenol conversion
x_{st}	steady state phenol conversion
z	axial coordinate (cm)

Greek letters

ε	bed porosity
ε_f	fixed bed porosity

et al. [13], and Vinod et al. [14], tested the degree of phenol biodegradation for different substrate concentrations and flow rates, obtaining removal percentages of about 90%. Puhakka et al. [15], studied the biodegradation of polychlorinated phenolic compounds using mixed cultures, celite supports and pure oxygen aeration.

In the above studies only the use of immobilized microorganisms for phenol removal was tested, but the corresponding mathematical models were not developed. Very few studies with immobilized microorganisms were found in which a mathematical model was proposed [16,17].

Enzymatic treatments have been presented as an alternative technology, since they can operate over wide pH and temperature ranges and have greater substrate specificity than microorganisms. Moreover, microorganisms produce a great amount of biomass that needs to be treated and even eliminated.

In recent years, free and immobilized peroxidases have been found to be viable alternatives in the phenol removal process, as can be observed from the great number of works published in this area [18–23]. In most of these studies free enzymes were used in discontinuous tank reactors, which made them impossible to reuse and eliminate from the bulk reaction.

The use of immobilized enzymes has several advantages. For instance, they can be easily separated from the reaction products and reused. They also work better in continuous processes [24–27].

Continuous processes with immobilized enzymes can be carried out in different reactor configurations, although fluidized bed reactors have certain advantages compared with the conventionally used tank and packed bed reactors. Fluidized beds are especially recommended when the substrates are viscous or contain suspended particles. The pressure drop is smaller when using fluidized bed reactors and the flow distribution through the reactor radial section is more uniform, which minimises the formation of preferential channels. Also, since mechanical stirring is not necessary, the support particles are less damaged by abrasion. All these advantages are of special interest in the phenol oxidation process using immobilized peroxidase, since most of the products formed are insoluble, which in packed bed reactors would lead to clogging phenomena and to an increase of the pressure drop.

However, despite the many papers published on the use of fluidized bed reactors for the removal of phenolic compounds with immobilized microorganisms, very a few works have used immobilized enzymes for the same purpose. Moreover, in the few studies that do exist, the enzyme was immobilized using physical methods, none having been found in which the immobilization process was carried out by covalent coupling. As regards published papers related to fluidized bed with immobilized peroxidases, Trivedi et al. [28], using soybean peroxidase entrapped on a hybrid silica/alginate gel, investigated phenol elimination in continuous in a fluidized bed reactor with recirculation. Also, Ensuncho et al. [29], used immobilized tyrosinase to catalyze the phenol conversion to *o*-quinones, in the presence of oxygen, in a three-phase fluidized bed reactor. In this study, the enzyme was physically retained in a mixed matrix of chitosan and alginate.

We have found no reference to the use of peroxidases immobilized by covalent coupling for the removal of phenol in fluidized bed reactors, nor any mathematical model for this process. However, for other processes, different fluidized bed reactor models have been used for systems involving enzymes covalently immobilized onto a solid support [30–34]. Some aspects of these models have been taken into account in the development of the reactor model described in the present work.

In this work, immobilized derivatives of soybean peroxidase covalently bound to glass supports with different surface areas, have been used, probably for the first time, in a fluidized bed reactor, in order to study their viability for phenol removal, as well as the influence of different operational variables. Since knowledge of phenol removal processes in fluidized bed reactors and their simulation is vital for designing a continuous industrial scale process, a reactor model, based on the experimental results that predicts the system's behaviour both in steady and transient state has been designed.

2. Experimental

2.1. Materials

Enzyme and substrates: soybean peroxidase enzyme (SBP) (EC 1.11.1.7, 108 IU/mg), catalase (EC 1.11.1.6, 2200 IU/mg) from bovine liver, hydrogen peroxide (35%, w/v), phenol (molecular mass 94.11, minimum purity 99%), were purchased from Sigma–Aldrich Fine Chemical.

Colorimetric reagents: 4-aminoantipyrine (AAP) and potassium ferricyanide, were purchased from Sigma–Aldrich Fine Chemicals.

Immobilization reagents: nitric acid (HNO_3) of 65% purity (Merck), γ-APTES ((3-aminopropyl) trietoxysilane) ($C_9H_{23}NO_3Si$), hydrochloric acid (HCl) of 36.5% purity (Probus S.A.) and glutaraldehyde ($OCH(CH_2)_3CHO$) of 25% purity.

Supports:

(a) PG 75-400: controlled pore glass 75-400, with a 200–400 mesh particle size, 77 Å average pore diameter and 182×10^4 cm^2/g surface area.
(b) PG 350-80: controlled pore glass 350-80, with a 20–80 mesh particle size, 350 Å average pore diameter and 53.45×10^4 cm^2/g surface area, purchased from Sigma–Aldrich.

2.2. Immobilization

Immobilized derivatives were prepared by covalent coupling between the amine groups of the protein and the aldehyde groups of the porous glass treated with (3-aminopropyl) triethoxysilane and glutaraldehyde, as in a previous work [35]. The immobilization procedure, protein determination and activity measurements are described below.

2.2.1. Immobilization procedure

During each immobilization, 5 g of support was the maximum amount that could be used. Using 1 g of support, the immobilization process was carried out according to the following steps:

- *Preparation of the carrier*: glass beads were washed in 5% HNO_3 at 80–90 °C for 60 min and then rinsed with distilled water and dried in an oven for 24 h at 110 °C.
- *Support activation*: to 1 g of clean PG, 18 ml of distilled water was added along with 2 ml of γ-APTES (10%, v/v) and the pH was adjusted to between pH 3 and 4 with 6N HCl. After adjustment, the mixture was placed in a 75 °C water bath for 2 h. The silanized glass was removed from the bath, washed with distilled water and dried overnight in an oven at 110 °C. The resulting product may be stored for later use.
- *Immobilization on PG-glutaraldehyde*: 1 g of silanized glass was made to react in a jacketed column reactor (3 i.d. and 40 cm length) with 25 ml of glutaraldehyde 2.5% in 0.05 M phosphate buffer, pH 7. The reactor was equipped with a porous glass plate placed 4.5 cm from the bottom. The solution was recycled for 60 min with a peristaltic pump and the PG-glutaraldehyde washed with 25 ml of the same buffer. Enzyme solution (40 ml of SBP 2 mg/ml solution) was then added to the reactor and the enzyme solution recycled overnight at 4 °C. The derivative was then washed three times with 0.1 M phosphate buffer, pH 7. The immobilized derivative was suspended in 50 ml of the same buffer and stored at 4 °C until use.

2.2.2. Protein determination

The amount of protein initially offered and in the wash-liquid after immobilization was determined by Lowry's procedure modified by Hartree [36], using bovine serum albumin as a standard. The amount of coupled peroxidase was the difference between the amount of the enzyme added initially and the amount of enzyme in the wash-liquid.

2.2.3. Activity measurements of free and immobilized enzyme

The initial reaction rates of both soluble and immobilized enzyme were measured in a jacketed batch reactor (50 ml total volume) at 30 °C and pH 7. Substrate concentrations (phenol and hydrogen peroxide) were kept constant at 2 mM, while enzyme concentration was varied between 0.01 and 0.05 mg/ml. Samples were taken from the reactor every 2.5 min and phenol concentration was determined as described below. When the immobilized enzyme derivatives were tested for activity, the samples were passed through a nylon membrane (10 μm) to retain the solid biocatalyst and phenolic polymer particles in the reactor. When the enzymes were used in solution, the samples from the reactor were poured into 1 ml of catalase solution (2200 IU ml^{-1}) to stop the reaction by breaking down the hydrogen peroxide. For this, 0.2 ml of a coagulant ($AlK(SO_4)_2$ 40 g l^{-1}) were added to 1 ml of the former mixture, before centrifuging for 30 min at $10{,}000 \times g$. With the activity data of free and immobilized enzyme, the activity yield was calculated.

Two immobilizations were carried out with PG 75-400 and another two with PG 350-80. The results obtained are shown in Table 1, where the more important characteristics of each derivative (immobilized protein (%), mg E/g support, mg E/ml storage suspension, activity yield (%) and IU/mg immobilized E) are reported. As can be seen in Table 1, the activity yield of the four derivatives was very similar, varying from 68 to 74%, which guaranties the possibility of using similar activities in the fluidized bed.

2.3. Analytical method

Phenol concentrations were measured by a colorimetric method using solutions of potassium ferricyanide (83.4 mM in 0.25 M sodium bicarbonate solution) and 4-aminoantipyrine (20.8 mM in 0.25 M sodium bicarbonate solution). Aliquots (2.4 ml) of the sample (phenol concentration up to 0.2 mM) were placed in a spectrophotometer cuvette (3 ml) together with 0.3 ml of ferricyanide solution and 0.3 ml AAP solution. After a few minutes to allow the colour to develop fully, absorbance was measured at 505 nm against a blank (2.4 ml of water, 0.3 ml ferricyanide solution and 0.3 ml AAP solution). Absorbance values were transformed to phenol concentrations in the sam-

Table 1
Immobilization results

Derivative	1	2	3	4
Support	PG 75-400	PG 75-400	PG 350-80	PG 350-80
Immobilized protein (%)	43.45	45.05	42.34	34.51
mg E/g support	34.76	36.04	33.87	27.61
mg E/ml storage suspension	0.695	0.721	0.677	0.552
Activity yield (%)	74.0	71.3	68.5	70.1
IU/mg immobilized E	79.9	77.0	74.0	75.7
IU/ml storage suspension	55.5	55.5	50.1	41.8

ple by using a calibration curve ($[\text{phenol}] = 0.0952 \times \text{Abs}_{505}$, $R = 0.9997$).

2.4. Experimental system and operational procedure

2.4.1. Experimental system

A jacketed glass column, two peristaltic pumps, two feeding tanks and a thermostatic bath are included in the experimental system. A schematic diagram is shown in Fig. 1. The reactor column had an internal diameter of 1 cm and a maximum useful height of 21 cm. A porous plate positioned 3 cm from the column bottom acted as liquid distributor. Water from the thermostatic bath maintained the reactor column at a constant temperature. A mesh was placed in the upper part of the column so that the immobilized biocatalyst could be fluidized and the reactor operates as a fluidized bed. Substrates (phenol and hydrogen peroxide) were pumped by two peristaltic pumps from the bottom to the top of the reactor, while the effluents with the reaction products were collected by overflow system, thus providing a constant volume in the reactor.

2.4.2. Operational procedure

In each assay, the reactor was charged with the required initial packed bed height. This operation was carried out as follows: a known volume was taken from the storage suspension containing the immobilized derivative, and placed inside the reactor. Once the catalytic particles were settled on the porous plate, the supernatant liquid was removed and the packed bed height was measured. This operation was repeated until the initial fixed bed height of the assay was achieved. From the total storage suspension volume added to the reactor and with the value of the mg E/ml storage suspension ratio, shown in Table 1, the total amount of enzyme in the bed was calculated.

Next, the reactor volume was completely filled with distilled water and the two peristaltic pumps of the substrate feed were connected simultaneously. The time course of the process was monitored by taking samples at the reactor outlet at regular time intervals.

2.5. Experimental planning

All the assays were carried out at 20 °C and pH 7. The substrates, phenol and hydrogen peroxide, were all aqueous solutions.

2.5.1. Bed height variation

Different values of initial bed height were used (0.5, 1.0, 1.5 and 2.0 cm) to determine the influence of this parameter on

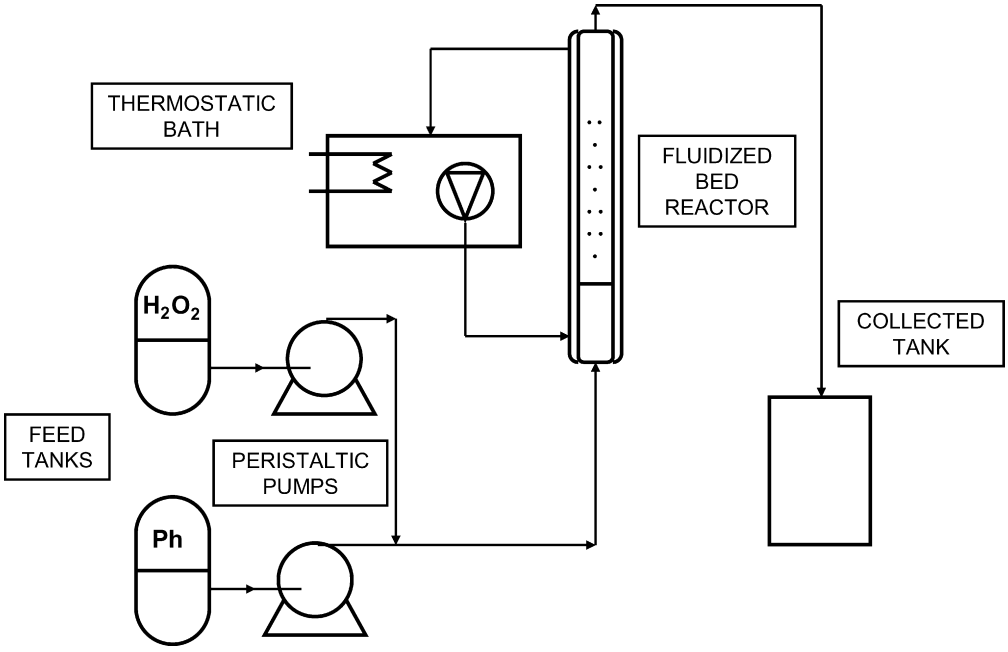

Fig. 1. Flow diagram of experimental equipment.

phenol removal. A fluidized bed reactor with both soybean peroxidase derivatives, PG 75-400 and PG 350-80, were used. The flow rate was kept constant at 5.0 ml/min, as was the substrate concentrations (phenol and hydrogen peroxide) at 1.0 mM. For this experimental series, derivatives 1 and 3 of Table 1 were selected.

2.5.2. Feed flow variation

Several experiments were carried out with both immobilized derivatives (PG 75-400 and PG 350-80), using three different feed flows: 5.0, 7.5 and 10.0 ml/min. In all the assays, substrate concentrations (phenol and hydrogen peroxide) were fixed at 1.0 mM and the initial fixed bed height at 1.5 cm. Derivatives 1 and 3 of Table 1 were also selected for this series.

2.5.3. Substrate concentrations variation

The influence of substrate concentrations (hydrogen peroxide and phenol) was studied in the fluidized bed reactor. Three substrate concentrations (0.5, 1.0 and 1.5 mM hydrogen peroxide and phenol, molar ratio 1:1) were assessed, using the same flow rate of 5.0 ml/min. A bed height of 1.0 cm was used with the PG 75-400 immobilized derivative and of 1.5 cm with the PG 350-80 derivative, because conversions obtained with this derivative with a 1.0 cm bed height were very small. Derivatives 2 and 4 of Table 1 were used in this experimental series.

3. Results and discussion

3.1. Results presentation

The experimentally measured variable was the phenol concentration in the effluent, denominated C_M in the design model shown below. The C_M value was normalized with respect to the phenol concentration in the feed flow, C_0, by defining a conversion, $x = (C_0 - C_M)/C_0$ (Eq. (32) of design model), which permitted the use of a scale varying from 0 to 1 in the plotting and also simplified the comparison between the different experimental series.

Since the reactor volume was initially filled with distilled water, the initial value of C_M was zero in all the assays and the initial conversion was always unity. After connecting the feed pumps, the C_M value increased continuously and the conversion decreased until the constant value corresponding to the steady state was reached. This can be observed from Figs. 2, 4 and 5, where the time course of the conversion was represented for the different experimental series.

It is important to note that, with the exception of the steady state, the conversion values shown in Figs. 2, 4 and 5 are not the exact values for the phenol fraction converted into products. In fact, although the apparent initial conversion is unity, the real conversion value must be zero at the beginning of the process since, at that time, there is no reaction because there are no substrates in the reactor. Thus, during the transient state, x is really a formal conversion, which equals the real conversion when the steady state is reached. For this reason, it is the steady state conversion that is used in the following discussion of the results.

3.2. Discussion

As regards the steady state conversion values, which are shown in Figs. 2, 4 and 5 in the horizontal region of the progress curve, it can be concluded that, if good percentages of phenol removal are to be reached, a high degree of activity should be attained in the bed, and a low flow rate and supports with a high specific surface area must be selected. For the optimal conditions of this work, phenol removal only reached about 80%. Higher values of specific surface area and/or effluent recycling should be used if higher removal percentages are to be reached.

When comparing the removal percentages obtained in this work with those reached in some of the studies cited in the Introduction, it can be concluded that the highest percentages of phenol removal are reached when immobilized microorganisms are used in the fluidized bed. However, the main disadvantage of this option was the high amount of biomass generated.

In the comments made in the Introduction section concerning the use of immobilized enzymes as catalyst in fluidized bed reactors, we mentioned the immobilization procedures used, which were always physical. However, in the present work we use an immobilization procedure involving covalent coupling to the support. Generally, the principal advantage of covalent immobilization is the higher operational stability of the derivative, which in continuous reactors, results in a longer operational time for the reactor. This happened with the derivatives used in this work, as can be seen from Figs. 2, 4 and 5, where, after 2 h operating, the steady state conversion value remained stable.

Figs. 2, 4 and 5 also show the influence of the different operational variables on the steady state conversion. These are discussed below.

3.2.1. Influence of initial bed height

In Fig. 2, variations in the conversion with reaction time are represented by dots for the different initial packed bed heights and for each support. It can be observed that when the bed height was increased, the maximum conversion increased for both immobilized derivatives (PG 75-400 and PG 350-80) because of the higher amount of immobilized derivative used, which results in greater enzyme activity in the bed.

However, for the same bed height, conversion was higher with SBP immobilized on PG 75-400 than on PG 350-80, perhaps because of the higher activity that SBP showed on this support for the same bed height (Table 2). On the other hand, differences in the conversion values, (approximately double for PG 75-400 than for PG 350-80), were much more pronounced than the differences between the amounts of enzyme activity (about 30% higher for PG 75-400 than for PG 350-80) in the bed. Taking into account that the surface area of the PG 75-400, 182×10^4 cm^2/g, was higher than that of the PG 350-80, 53.45×10^4 cm^2/g, external diffusion control phenomena could have occurred, a hypothesis that agrees with the differences observed in the conversion values. To check this hypothesis, the steady state conversion values for both supports, calculated as the average conversion obtained between 60 and 120 min, were plotted against the amount of enzyme activity corresponding to each bed height (Fig. 3). In this figure it is observed that, for

Table 2
Correspondence between the amount of SBP (mg and I.U.) on each support and the different bed heights

Fixed bed height (cm)	PG 75-400		PG 350-80	
	SBP (mg)	SBP (IU)	SBP (mg)	SBP (IU)
0.5	6.459	516.2	4.988	369.0
1.0	12.919	1032.5	9.976	738.0
1.5	19.378	1548.7	14.964	1107.0
2.0	25.837	2064.9	19.951	1476.0

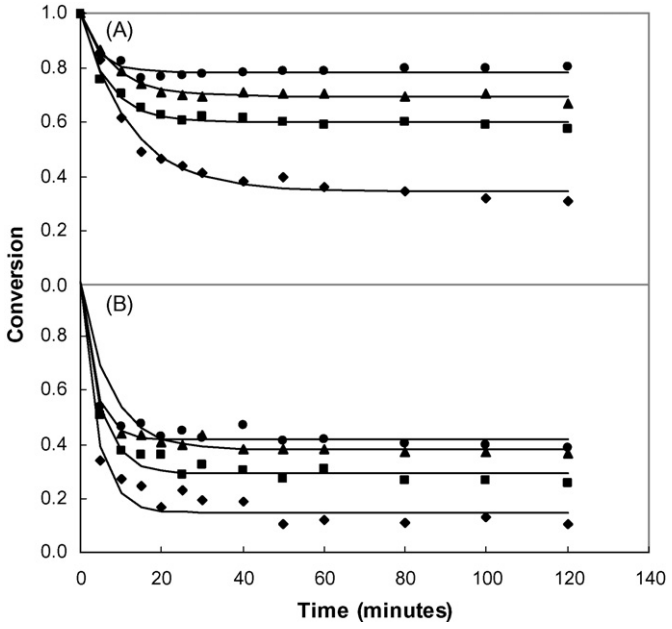

Fig. 2. Time course of phenol conversion and data fitting to model for different bed heights: (A) PG 75-400 and (B) PG 350-80. Bed height: (●) 2 cm, (▲) 1.5 cm, (■) 1 cm, (♦) 0.5 cm, (—) model.

similar amounts of enzyme activity, the conversion values were almost double that obtained when PG 75-400 support was used.

Data from Fig. 3 were fitted to a polynomial function (continuous lines in the figure) and conversion data were estimated for equal values of enzyme activity in the bed. Since the flow rate in this series was kept constant at 5 ml/min, the estimated data correspond to equal values of the (effluent volume)/(catalyst activity) ratio. The estimated values for the steady state conversion, for three values of enzyme activity (500, 1000 and 1500 IU), were 0.32, 0.55 and 0.70, for PG 75-400, and 0.19, 0.33 and 0.42, for PG 350-80, respectively. The values obtained for PG 75-400 were approximately 66% higher than those corresponding to the same activity for PG 350-80, which confirms the influence of the specific surface area of the support and the existence of external diffusional limitations in the reaction process.

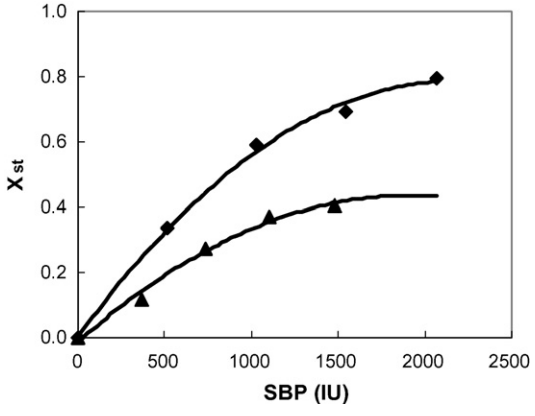

Fig. 3. Variation of steady state conversion with the amount of SBP activity (IU) in the fluidized bed: (♦) PG 75-400 and (▲) PG 350-80.

3.2.2. *Influences of flow rate*

In Fig. 4, variations in the conversion are plotted against time for both supports at three different flow rates: 5.0, 7.5 and 10.0 ml/min. A increase in the flow rate resulted in both a decrease in spatial time and a decrease in the amount of phenol conversion, as was expected.

In this series, the bed height was kept constant at 1.5 cm, so that it contained 1548.7 SBP (IU) for the PG 75-400 derivative and 1107.0 SBP (IU) for the PG 350-80. The higher conversion reached by the former system may be attributed to the higher amount of SBP activity on this support. However, the observed differences were very pronounced since, with approximately 30% more enzyme activity in the bed, the conversions achieved with PG 75-400 were approximately double that obtained with

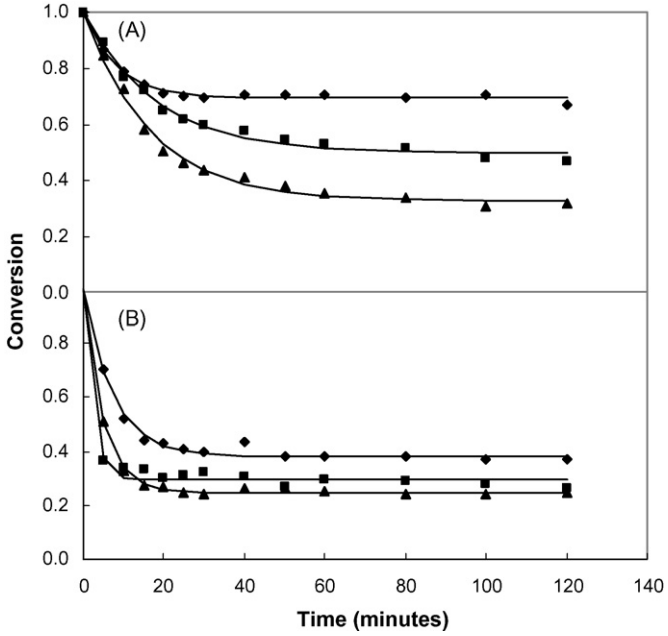

Fig. 4. Time course of phenol conversion and data fitting to model for different flow rates: (A) PG 75-400 and (B) PG 350-80. Flow rate: (♦) 5 ml/min, (■) 7.5 ml/min, (▲) 10 ml/min, (—) model.

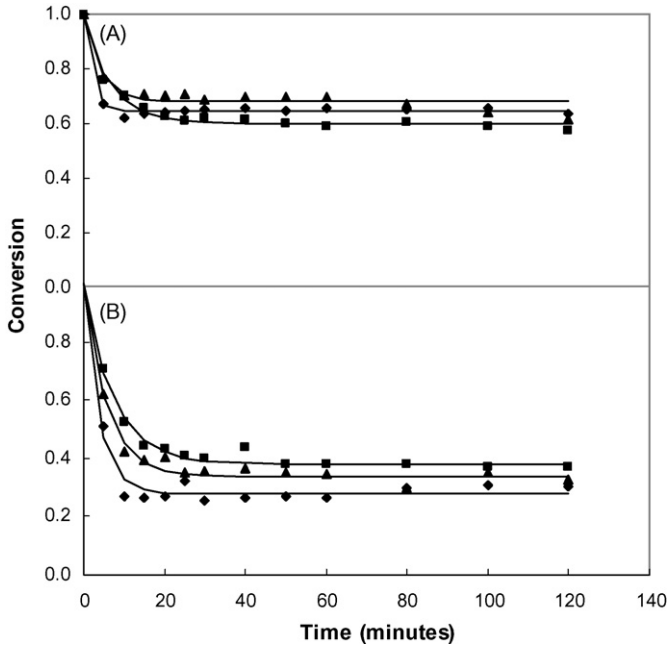

Fig. 5. Time course of phenol conversion and data fitting to model for different substrate concentrations: (A) PG 75-400 and (B) PG 350-80. Substrate concentrations: (♦) 0.5 mM, (■) 1 mM and (▲) 1.5 mM, (—) model.

PG 350-80, showing, once again, the influence of the surface area of the support and the presence of external diffusional limitations.

3.2.3. Influence of initial substrate concentrations

The results obtained are given in Fig. 5, where the conversion is plotted against time for both supports, three substrate concentrations (0.5, 1.0 and 1.5 mM) and a molar ratio of 1:1. It is observed that, similar conversion percentages were obtained when substrate concentration was varied, which leads us to affirm again the existence of a diffusional control because, in these conditions, the process rate follows a first order law and the conversion is independent of the initial concentration.

On the other hand, in this series different bed heights were used for each support. The bed height of 1.0 cm used for PG 75-400 (derivative 2) contained 1031.4 IU of SBP, while the 1.5 cm height used for PG 350-80 (derivative 4) contained 1165.3 IU of SBP. In spite of the greater amount of enzyme activity in the bed, the conversions reached with the PG 350-80 support were again lower than to those reached with the SBP immobilized in PG 75-400, which can be attributed to the smaller surface area of PG 350-80.

The existence of a diffusional control of the process was therefore confirmed with the different experimental series and a model, based on this control of the external diffusion, was formulated.

4. Fluidized bed: model as pfr and in-series mixer

4.1. Model hypothesis

- The reactor is considered equivalent to a fluidized bed in series with a ideal mixer.
- For the fluidized bed, the plug flow hypothesis is accepted.
- In each experiment, the porosity, ε, is constant and uniform along the bed, because the flow rate, F, remains constant.
- The reaction takes place on the surface of the catalytic particles. The high enzyme/substrate ratio in the bed means that the biochemical reaction is faster than the diffusion of the substrates from the bulk solution to the surface of the catalytic particles. The process is controlled by the external diffusion and the overall rate is given by the equation: $r = -k_L a_s (C - C^*)$
- The substrate is consumed quickly on the catalytic bead surface, and so the approximation $C \gg C^*$ can be made. Therefore, the rate equation can be reduced to $r = -k_L a_s C$, which determines a first order kinetic law with respect to the substrate concentration.
- The reactor volume existing after the fluidized bed acts as an ideal mixer. There is no reaction in the mixer because there are no catalytic particles inside, but the continuous movement of the polymer particles in that region will mix the effluent from the fluidized bed with the liquid present in the mixing zone.

4.2. Mass balance in the fluidized bed

Taking into account an elemental volume, $\Delta V = A\Delta z$, where A is the normal bed section and z the axial coordinate, an instantaneous substrate mass balance gives the following equation:

$$(FC)_{z+\Delta z} - (FC)_z + \varepsilon A \Delta z \frac{\partial C}{\partial t} + (1-\varepsilon) A \Delta z k_L a_s C = 0 \quad (1)$$

Dividing by Δz, and for the limit when $\Delta z \to 0$, the following equation is obtained:

$$\frac{\partial (FC)}{\partial z} + \varepsilon A \frac{\partial C}{\partial t} + (1-\varepsilon) A k_L a_s C = 0 \quad (2)$$

For constant F, Eq. (2) can be written as

$$\frac{F}{\varepsilon A}\frac{\partial C}{\partial z} + \frac{\partial C}{\partial t} + \frac{(1-\varepsilon)}{\varepsilon} k_L a_s C = 0 \quad (3)$$

Defining

$$v = \frac{F}{\varepsilon A}; \qquad k = \frac{(1-\varepsilon)}{\varepsilon} k_L a_s \quad (4)$$

the following mass balance differential equation is obtained:

$$\frac{\partial C}{\partial t} + v\frac{\partial C}{\partial z} + kC = 0 \quad (5)$$

with the initial and boundary conditions

$$0 \le z \le L, \quad t = 0, \quad C(z, 0) = 0 \quad (6)$$

$$z = 0, \quad t > 0, \quad C(0, t) = C_0 \quad (7)$$

4.3. Mass balance in the mixer

For the mixer, an instantaneous substrate mass balance gives the following equation:

$$FC_M - FC_L + V_M \frac{\partial C_M}{\partial t} = 0 \tag{8}$$

where C_L is the outlet substrate concentration from the fluidized bed, L the length, C_M the substrate concentration in the mixer and V_M the volume.

Reordering Eq. (8), gives Eq. (9)

$$\frac{\partial C_M}{\partial t} + \frac{F}{V_M} C_M = \frac{F}{V_M} C_L \tag{9}$$

with the initial condition

$$t = 0, \quad C_M = 0 \tag{10}$$

5. Solving the model

5.1. Fluidized bed solution

5.1.1. Steady state

For the steady state, ($t \to \infty$), Eq. (5) reduces to

$$v \frac{dC}{dz} + kC = 0 \tag{11}$$

with the condition

$$z = 0, \quad C = C_0 \tag{12}$$

The solution is

$$C = C_0 \, e^{-(k/v)z} \tag{13}$$

Therefore, it can be established that

$$\lim_{t \to \infty} C(z, t) = C_0 \, e^{-(k/v)z} \tag{14}$$

5.1.2. Transient state

For the transient state, the following solution is proposed:

$$C = C_0 e^{-(k/v)z}(1 - f(z, t)) \tag{15}$$

Taking into account Eqs. (6) and (7), the conditions for $f(z, t)$ are

$$f(z, 0) = 1 \tag{16}$$

$$f(0, t) = 0 \tag{17}$$

From Eq. (15), the derivatives of $C(z, t)$ will be given by

$$\frac{\partial C}{\partial t} = -C_0 \, e^{-(k/v)z} \frac{\partial f}{\partial t} \tag{18}$$

$$\frac{\partial C}{\partial z} = -\frac{k}{v} C_0 \, e^{-(k/v)z}(1 - f) - C_0 \, e^{-(k/v)z} \frac{\partial f}{\partial z} \tag{19}$$

Substituting Eqs. (18) and (19) into Eq. (5), and simplifying, the differential equation for $f(z, t)$ is obtained

$$\frac{\partial f}{\partial t} + v \frac{\partial f}{\partial z} = 0 \tag{20}$$

with the conditions given by Eqs. (16) and (17).

Applying Laplace's transform to Eq. (20) to eliminate the time variable, and representing $Lf(z, t)$ by $f(z, s)$, gives

$$sf(z, s) - 1 + v \frac{df(z, s)}{dz} = 0 \tag{21}$$

Applying Laplace's transform again to Eq. (21) to eliminate the z variable, we finally obtain

$$sf(p, s) - \frac{1}{p} + vpf(p, s) = 0 \tag{22}$$

From Eq. (22)

$$f(p, s) = \frac{1/v}{p((s/v) + p)} \tag{23}$$

which in simple fractions, can be expressed as

$$f(p, s) = \frac{1}{s} \left(\frac{1}{p} - \frac{1}{(s/v) + p} \right) \tag{24}$$

The inverse transform with respect p gives

$$f(z, s) = \frac{1}{s} - \frac{e^{-(s/v)z}}{s} \tag{25}$$

and, restoring the t variable, the final solution is obtained

$$f(z, t) = 1 - U\left(t - \frac{z}{v}\right) \tag{26}$$

where

$$U\left(t - \frac{z}{v}\right) = 0 \quad \text{for } t \leq \frac{z}{v} \tag{27}$$

$$U\left(t - \frac{z}{v}\right) = 1 \quad \text{for } t > \frac{z}{v} \tag{28}$$

and the complete transient solution for the fluidized bed is

$$C(z, t) = C_0 \, e^{-(k/v)z} U\left(t - \frac{z}{v}\right) \tag{29}$$

Not only is the steady state solution reached when $t \to \infty$ but also from the moment that the condition expressed in Eq. (28) is fulfilled.

5.1.3. Concentration at the end of the fluidized bed

The concentration is given by Eq. (29) when $z = L$. Because the sample time interval used in the experiments fulfils the condition expressed in Eq. (28), it can be affirmed that

$$C(L, t) = C_0 \, e^{-(k/v)L} \tag{30}$$

throughout the experiment and for the different individual times, except for the initial value $t = 0$, when $C(L, t) = 0$.

5.2. Mixer zone solution

From the above solution obtained for the fluidized bed, it can be deduced that the outlet concentration, C_L, is a constant value (zero or the value given by Eq. (30)), which facilitates integration of the mixer zone differential equation, to give

$$C_M(t) = C_0 \, e^{-(k/v)L}(1 - e^{-(F/V_M)t}) \tag{31}$$

Defining the conversion as

$$x = \frac{C_0 - C_M}{C_0} \tag{32}$$

it follows that

$$x(t) = 1 - e^{-(k/v)L}(1 - e^{-(F/V_M)t}) \tag{33}$$

For the steady state, Eq. (33) reduces to

$$x_{st} = 1 - e^{-(k/v)L} \tag{34}$$

which indicates that the following relationship is verified:

$$\ln(1 - x_{st}) = -\frac{k}{v}L \tag{35}$$

This is confirmed when the model is checked (see below).

6. Checking the model

6.1. Steady state

Eq. (35) was checked with the steady state conversion values, x_{st}, obtained experimentally as the average conversion attained between 60 and 120 min. In this equation, the fluidized bed length, L, can be expressed as a simple function of the initial fixed bed length, L_f, and the bed porosity, ε, according to the following equation:

$$(1 - \varepsilon)L = (1 - \varepsilon_f)L_f \tag{36}$$

Taking into account, also, Eq. (4) for k and v, Eq. (35) can be written as

$$\ln(1 - x_{st}) = -(1 - \varepsilon_f)Ak_L a_s \frac{L_f}{F} \tag{37}$$

Considering that L_f and F are known operational conditions for all the experiments, and ε_f and A are constant values, a graph of $\ln(1 - x_{st})$ with the inverse of F should be a straight line. Fig. 6 is the representation of Eq. (37) for the L_f variable, F variable and C_0 variable series and the two immobilized derivatives. As can be seen, steady state conversions are very close to the behaviour expressed in Eq. (37). Furthermore, if the same value of ε_f is assumed for the two immobilized derivatives, the slope of the straight lines represented in Fig. 6 should be proportional to the surface area of the catalytic particles, which is confirmed in Fig. 7.

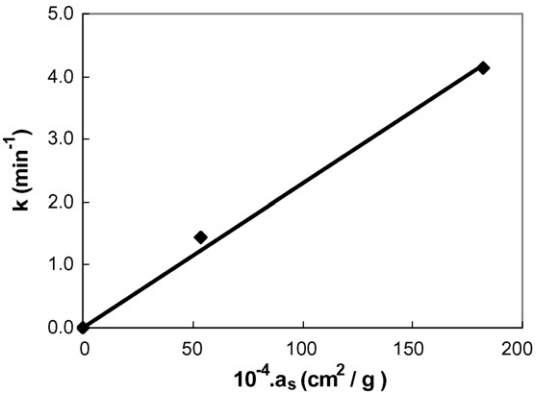

Fig. 7. Dependence of k on specific surface area.

6.2. Transient state

For the transient state, the solution given by Eq. (33), together with the steady state conversion value given by Eq. (34), follow the relationship:

$$x(t) = 1 - (1 - x_{st})(1 - e^{-(F/V_M)t}) \tag{38}$$

which can be written as

$$x(t) = 1 - (1 - a)(1 - e^{-bt}) \tag{39}$$

This equation has two unknown parameters, a and b, which can be determined by fitting. Experimental values of $x(t)$ for all the experiments were fitted to Eq. (39), using the CurveExpert V 3.1 software; the values obtained for a and b, together with the statistical parameters regression coefficient, R, and standard deviation, S.D., are included in Table 3. With the values of a and b obtained, and using Eq. (39), theoretical values of $x(t)$ were estimated. The continuous lines in Figs. 2, 4 and 5 are the calculated values of $x(t)$ and the dots the experimental values for the three experimental series. Furthermore, Fig. 8 shows the calculated values of the steady state conversion given by the

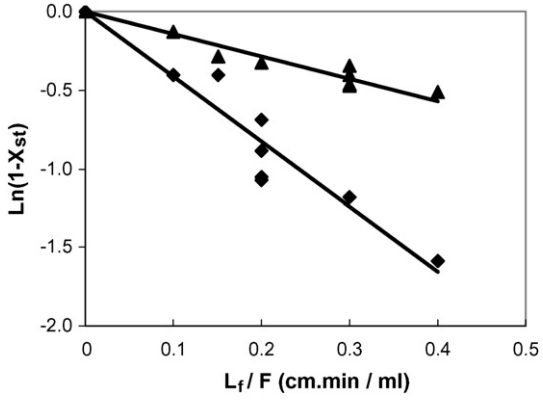

Fig. 6. Fitting of steady state conversion to Eq. (37): (♦) PG 75-400 and (▲) PG 350-80.

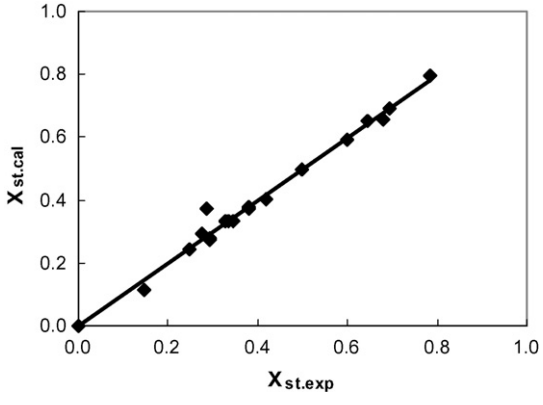

Fig. 8. Comparison between experimental and calculated steady state conversions for both PG 75-400 and PG 350-80 supports.

Table 3
Model parameters and statistics

Support	Co (mM)	F (ml/min)	L_f (cm)	a	b	R	S.D.
PG 75-400	1.0	5.0	0.5	0.346	0.082	0.991	0.029
PG 75-400	1.0	5.0	1.0	0.601	0.153	0.991	0.016
PG 75-400	1.0	5.0	1.5	0.695	0.123	0.993	0.012
PG 75-400	1.0	5.0	2.0	0.784	0.231	0.974	0.015
PG 75-400	1.0	10.0	1.5	0.327	0.060	0.997	0.019
PG 75-400	1.0	7.5	1.5	0.498	0.055	0.995	0.017
PG 75-400	1.0	5.0	1.5	0.695	0.123	0.993	0.012
PG 75-400	0.5	5.0	1.0	0.645	0.555	0.994	0.011
PG 75-400	1.0	5.0	1.0	0.601	0.153	0.991	0.016
PG 75-400	1.5	5.0	1.0	0.681	0.243	0.991	0.027
PG 350-80	1.0	5.0	0.5	0.148	0.249	0.977	0.050
PG 350-80	1.0	5.0	1.0	0.292	0.214	0.989	0.030
PG 350-80	1.0	5.0	1.5	0.381	0.137	0.994	0.020
PG 350-80	1.0	5.0	2.0	0.418	0.283	0.980	0.032
PG 350-80	1.0	10.0	1.5	0.248	0.214	0.999	0.009
PG 350-80	1.0	7.5	1.5	0.294	0.434	0.992	0.025
PG 350-80	1.0	5.0	1.5	0.381	0.137	0.994	0.020
PG 350-80	0.5	5.0	1.5	0.277	0.263	0.990	0.029
PG 350-80	1.0	5.0	1.5	0.285	0.203	0.993	0.023
PG 350-80	1.5	5.0	1.5	0.336	0.173	0.991	0.027

a parameter, and the experimental value. Finally, Fig. 9 is an overall comparison between the calculated and the experimental values of $x(t)$, for all the experimental series and times. The excellent fit obtained (better with the smaller particles) leads us to conclude that the model is valid as a predictive model for the reactor considered.

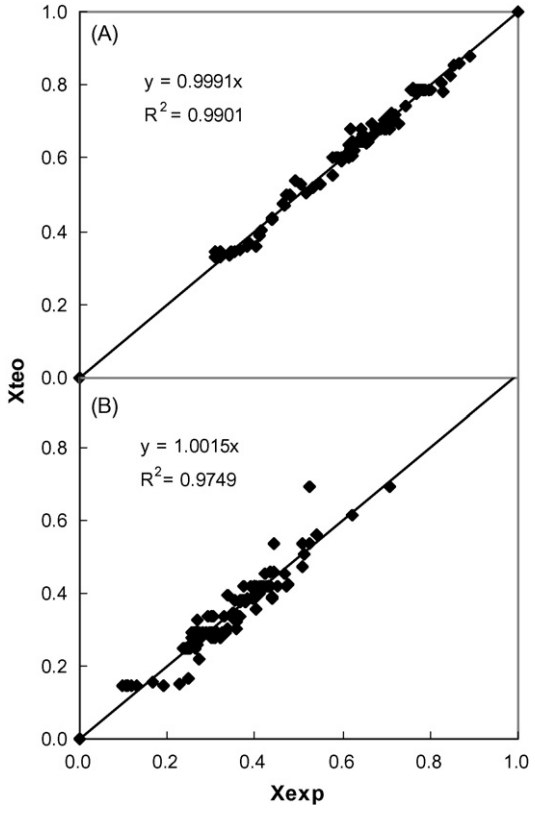

Fig. 9. Comparison between calculated and experimental conversions for all data series and the two supports: (A) PG 75-400 and (B) PG 350-80.

Acknowledgements

This work was supported by a grant, 00505/PI/04, from Fundación Séneca (Comunidad Autónoma de la Región de Murcia), Spain. During the time that this study was being carried out, M. Dolores Murcia was a beneficiary of a scholarship from this foundation, and María Gómez had a FPU scholarship from the Spanish Ministry of Education and Culture.

References

[1] A. Bhunia, S. Durani, P.P. Wangikar, Horseradish peroxidase catalyzed degradation of industrially important dyes, Biotechnol. Bioeng. 72 (2001) 562–567.
[2] G. Feijoo, J.M. Lema, Treatment of forest industry effluents with toxic and recalcitrant compounds by white-rot fungi, Afinidad 52 (1995) 171–180.
[3] M.S. Kumar, A.N. Vaidya, N. Shivaraman, A.S. Bal, Biotreatment of oil-bearing coke-oven wastewater in fixed-film reactor: a viable alternative to activated sludge process, Environ. Eng. Sci. 17 (2000) 221–226.
[4] M. Wagner, J.A. Nicell, Treatment of a foul condensate from Kraft pulping with horseradish peroxidase and hydrogen peroxide, Water Res. 35 (2001) 485–495.
[5] N.R. Khalili, J.D. Vyas, W. Weangkaew, S.J. Westfall, S.J. Parulekar, R. Sherwood, Synthesis and characterization of activated carbon and bioactive adsorbent produced from paper mill sludge, Sep. Purif. Technol. 26 (2002) 295–304.
[6] K. Loh, S. Ranganath, External-loop fluidized bed airlift bioreactor (EFBAB) for the cometabolic biotransformation of 4-chlorophenol (4-cp) in the presence of phenol, Chem. Eng. Sci. 60 (2005) 6313–6319.
[7] L. Shangen, Fermentation characteristics in high-concentration phenol wastewater treatment with the fluidized-bed granular activated carbon (GAC) anaerobic reactor, Huanjing Wuran Yu Fangzhi 15 (2) (1993) 13–17.
[8] M.T. Suidan, J.R.V. Flora, T.K. Boyer, A.M. Wuellner, B. Narayanan, Anaerobic dechlorination using a fluidized-bed GAC reactor, Water Res. 30 (1) (1996) 160–170.
[9] A. Hirata, M. Noguchi, N. Takeuchi, S. Tsuneda, Kinetics of biological treatment of phenolic wastewater in three-phase fluidized bed containing biofilm and suspended sludge, Water Sci. Technol. 38 (8/9) (1998) 205–212.

[10] K. Loh, J. Liu, External loop inversed fluidized bed airlift bioreactor (EIFBAB) for treating high strength phenolic wastewater, Chem. Eng. Sci. 56 (2001) 6171–6176.
[11] C. Juárez-Ramírez, N. Ruiz-Ordaz, E. Cristiani-Urbina, J. Mayer, Degradation kinetics of phenol by immobilized cells of Candida tropicalis in a fluidized bed reactor, World J. Microbiol. Biotechnol. 17 (2001) 697–705.
[12] G. González, M.G. Herrera, M.T. García, M.M. Peña, Biodegradation of phenol in a continuous process: comparative study of stirred tank and fluidized-bed bioreactors, Bioresour. Technol. 76 (3) (2001) 245–251.
[13] G. González, G. Herrera, M.T. García, M. Peña, Biodegradation of phenolic industrial wastewater in a fluidized bed bioreactor with immobilized cells of *Pseudomonas putida*, Bioresour. Technol. 80 (2) (2001) 137–142.
[14] A.V. Vinod, G.V. Reddy, Simulation of biodegradation process of phenolic wastewater at higher concentrations in a fluidized-bed bioreactor, Biochem. Eng. J. 24 (2006) 1–10.
[15] J.A. Puhakka, K. Järvinen, Aerobic fluidized-bed treatment of polychlorinated phenolic wood preservative constituents, Water Res. 26 (6) (1992) 765–770.
[16] S. Pallerla, R.P. Chambers, Reactor development for biodegradation of pentachlorophenol, Catal. Today 40 (1998) 103–111.
[17] A.V. Vinod, G.V. Reddy, Mass transfer correlation for phenol biodegradation in fluidized bed bioreactor, J. Hazard. Mater. 136 (3) (2006) 727–734.
[18] A. Bódalo, J.L. Gómez, E. Gómez, M. Gómez, M.D. Murcia, E. Sánchez, Removing chlorophenol with horseradish peroxidase immobilized on porous glass, in: Proccedings of the Fourth European Congress of Chemical Engineering (Short paper book), Spain, 2003.
[19] J.L. Gómez, A. Bódalo, E. Gómez, A.M. Hidalgo, M. Gómez, A new method to estimate intrinsic parameters in the ping-pong bisubstrate kinetics: application to the oxipolymerization of phenol, Am. J. Biochem. Biotechnol. 1 (2) (2005) 115–120.
[20] M.A. Duarte-Vázquez, M.A. Ortega-Tovar, B.E. García-Almendárez, C. Regalado, Removal of aqueous phenolic compounds from a model system by oxidative polymerization with turnip (*Brassica napus* L. var purple top white globe) peroxidase, J. Chem. Technol. Biotechnol. 78 (2003) 42–47.
[21] J.A. Nicell, Kinetics of horseradish peroxidase-catalyzed polymerization and precipitation of aqueous 4-chlorophenol, J. Chem. Technol. Biotechnol. 60 (1994) 203–215.
[22] K.E. Taylor, J.K. Bewtra, N. Biswas, Enzymatic treatment of phenolic and other aromatic compounds in wastewaters, in: Water Environmental Federation, 71st Annual Conference, Proceeding, vol. 3, Alexandria, VA, 1998, pp. 349–360.
[23] Y. Wu, K. Taylor, N. Biswas, J.K. Bewtra, Kinetic model-aided reactor design for peroxidase-catalyzed removal of phenol in the presence of polyethylene glycol, J. Chem. Technol. Biotechnol. 74 (1999) 519–526.
[24] I. Chibata, Immobilized Enzymes: Research and Development, John Wiley & Sons, New York, 1978.
[25] Q. Husain, U. Jan, Detoxification of phenols and aromatic amines from polluted wastewater by using phenol oxidases, J. Sci. Ind. Res. 59 (2000) 286–293.
[26] F. Rojas-Melgarejo, J.N. Rodríguez-López, F. García-Cánovas, P.A. García-Ruiz, Stability of horseradish peroxidase immobilized on different cinnamic carbohydrate esters, J. Chem. Technol. Biotechnol. 79 (2004) 1148–1154.
[27] K. Tatsumi, S. Wada, H. Ichikawa, Removal of chlorophenols from wastewater by immobilized horseradish peroxidase, Biotechnol. Bioeng. 51 (1996) 126–130.
[28] U.J. Trivedi, A.S. Bassi, J. Zhu, Investigation of continuous phenol removal in a liquid-solid circulating fluidized bed (LSCFD) using immobilized soybean seed hull peroxidases, in: Proceedings of the Seventh World Congress of Chemical Engineering, Glasgow, UK, 2005.
[29] L. Ensuncho, M. Alvarez-Cuenca, R.G. Legge, Removal of aqueous phenol using immobilized enzymes in a bench scale and pilot scale three-phase fluidized bed reactor, Bioprocess Biosyst. Eng. 27 (2005) 185–191.
[30] A. Bódalo, J.L. Gómez, E. Gómez, J. Bastida, M.F. Máximo, Modelo de diseño y simulación de reactores de lecho fluidizado con enzimas inmovilizadas, Afinidad 453 (1994) 341–348.
[31] A. Bódalo, J.L. Gómez, E. Gómez, J. Bastida, M.F. Máximo, Fluidized bed reactor operating with immobilized enzyme systems: design model and its experimental verification, Enzyme Microb. Technol. 17 (1995) 915–922.
[32] M. Hamdame, A.M. Wilhem, J.P. Riba, Modelling of a fluidized bed immobilized enzyme reactor. Application to the hydrolysis of maltodextrins, Chem. Eng. J 39 (2) (1988) B25–B30.
[33] T.D. Papathanasiou, N. Kalogerakis, L.A. Behie, Dynamic modelling of mass transfer phenomena with chemical reaction in immobilized-enzyme bioreactors, Chem. Eng. Sci. 43 (7) (1988) 1489–1498.
[34] M. Asif, A.E. Abasaeed, Modelling of glucose isomerization in a fluidized bed immobilized enzyme bioreactor, Bioresour. Technol. 64 (1998) 229–235.
[35] J.L. Gómez, A. Bódalo, E. Gómez, J. Bastida, A.M. Hidalgo, M. Gómez, Immobilization of peroxidases on glass beads: an improved alternative for phenol removal, Enzyme Microb. Technol. 39 (2006) 1016–1022.
[36] E.F. Hartree, Protein determination: an improved modification of Lowry's method which gives a linear photometric response, Anal. Biochem. 42 (1972) 422–427.